

Band offset in GaAs/Al_xGa_{1-x}As multiple quantum wells calculated with the *sp*³*s** tight-binding model

Y. Fu

Department of Physics and Measurement Technology, University of Linköping, S-58183 Linköping, Sweden

K. A. Chao

Institute of Physics, University of Trondheim, Norwegian Institute of Technology, N-7034 Trondheim, Norway

(Received 9 August 1990)

By incorporating a block-decimation method to the *sp*³*s** tight-binding model, we have studied the evolution of Al_xGa_{1-x}As electronic band structure as a function of Al composition, including the compositional correlation effect. Using the experimental data of a GaAs/AlAs multiple quantum well, we obtain the band edges of an Al_xGa_{1-x}As alloy as functions of *x*, from which the band offsets Δ*E*_V and Δ*E*_C as well as the band-offset coefficient $Q = \Delta E_C / (\Delta E_C + \Delta E_V)$ are derived for arbitrary Al concentration. The result agrees well with experiment.

I. INTRODUCTION

The effective-mass approximation (EMA) has been extensively used to study the energy-level structures of heterostructures, quantum wells, and semiconductor superlattices. Two key problems emerge in the case of the EMA. Because of the spatial dependence of the effective mass *m*(*z*) along the direction perpendicular to the interfaces (defined as the *z* axis), the *z* component of the kinetic-energy operator has the general form

$$\frac{1}{2} [m(z)]^\alpha \left[-i\hbar \frac{d}{dz} \right] [m(z)]^\beta \left[-i\hbar \frac{d}{dz} \right] [m(z)]^\alpha,$$

where $2\alpha + \beta = -1$. It is generally accepted that for GaAs/Al_xGa_{1-x}As multiple quantum wells (MQW), the most reasonable choice for the value of β is β = -1.

The second problem is related to the abrupt change of the potential function across the interface between any two different materials. Consider the type-I semiconductor superlattice GaAs/Al_xGa_{1-x}As as an example. The variation of the conduction-band minimum (or valence-band maximum) along the *z* axis is schematically shown in Fig. 1 as an array of square-well barriers. The conduction (or valence) -band offset Δ*E*_C (or Δ*E*_V) is important not only for the device design, but also for theoretical analysis, because the EMA Schrödinger equation can be reduced to one dimensional along the *z* axis with the potential *V*(*z*) identical to the square-well barriers given in Fig. 1. Conventionally, the band-offset coefficient is defined as

$$Q \equiv \Delta E_C / (\Delta E_C + \Delta E_V) = \Delta E_C / \Delta E_g, \tag{1}$$

where Δ*E*_g is the difference between the energy gap of the bulk Al_xGa_{1-x}As and the energy gap of bulk GaAs.

In Al_xGa_{1-x}As alloy the conduction-band minimum is at the Γ point if the Al composition *x* ≤ 0.38 but at the X point if *x* > 0.38, while the valence-band maximum is always at the Γ point for all values of *x*. Also for some

other practical reasons, the Al concentration of the usual device materials is either *x* ≤ 0.38 or *x* = 1.0. Therefore the direct measurements of the band offsets are quite restricted. In 1980, the *C-V* measurements at the abrupt GaAs/Al_xGa_{1-x}As heterojunctions¹ yielded a conduction-band offset Δ*E*_C ≈ 0.248 eV for *x* = 0.3.¹ The recent experimental values of Δ*E*_V on the molecular-beam-epitaxy-grown AlAs/GaAs [001] (*x* = 1) samples are Δ*E*_V = 0.45–0.56 eV,²⁻⁴ 0.535 ± 0.0125 eV,⁵ and 0.560 ± 0.03 eV.⁶

In the EMA the subband structures of a MQW system vary with the value of *Q* used in the calculation. *Q* can then be determined theoretically by fitting the computed excitation energies to the optical measurements. While the first value⁷ so obtained is *Q* ~ 0.9, the commonly accepted value now⁸ is *Q* ~ 0.6. Beyond the standard fitting procedure, there are also theoretical attempts⁹⁻²¹ to calculate Δ*E*_C or Δ*E*_V. Unfortunately, these theoretical studies did not lead to a unique conclusion.

Incorporating the measured value of Δ*E*_V for GaAs/AlAs (*x* = 1) to the *sp*³*s** tight-binding band calculation,²² the effect of microstructure order on the band gap of the Al_xGa_{1-x}As alloy for various alloy composition was obtained earlier.²³ In the present paper we im-

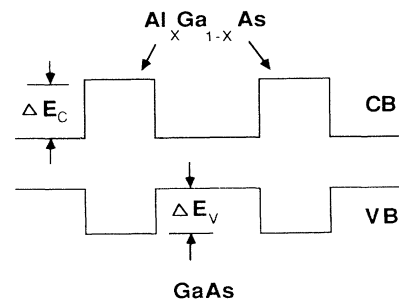


FIG. 1. A schematic illustration of the one-dimensional square-well barrier model for a GaAs/Al_xGa_{1-x}As MQW.

prove the calculation of Ref. 23 with a real-space renormalization scheme. While the sp^3s^* tight-binding model is outlined in Sec. II, the role of microstructure will be emphasized. The effective quasi-one-dimensional Schrödinger equation so derived will be solved analytically in Sec. III after a one-step block decimation. In Sec. IV we give the numerical result of the band edges of the $\text{Al}_x\text{Ga}_{1-x}\text{As}$ alloy, from which the band offsets ΔE_C and ΔE_V for arbitrary values of x are easily deduced. The computed band-offset coefficients for various microstructure orderings will then be compared with available experimental data. The weak points in the present calculation and its possible improvement are remarked in the last section, Sec. V.

II. sp^3s^* TIGHT-BINDING MODEL FOR SEMICONDUCTOR ALLOYS

Using Löwdin orbitals to perform a nearest-neighbor tight-binding band calculation, one needs to know the Hamiltonian matrix element $h_{\alpha\beta}^{ij}$ between the α th orbital on the i th atomic site $|i,\alpha\rangle$ and the β th orbital on the j th atomic site $|j,\beta\rangle$, where either $i=j$ or i is a nearest neighbor of j . For an $\text{Al}_x\text{Ga}_{1-x}\text{As}$ alloy, there are three different types of atom (Al, Ga, and As) and two different types of nearest-neighbor pair (Al-As and Ga-As). Assuming that any matrix element $h_{\alpha\beta}^{ij}$ in the $\text{Al}_x\text{Ga}_{1-x}\text{As}$ alloy has the same value as the corresponding matrix element in the pure bulk AlAs or bulk GaAs, we can use the results of Vogl *et al.*²² to derive the energy band structure. Vogl *et al.* have used five Löwdin orbitals sp^3s^* to calculate the energy band structures of pure bulk covalent semiconductors. For each semiconductor, the matrix elements $h_{\alpha\beta}^{ij}$ are determined semiempirically, and are listed in Ref. 22. In these calculations, each individual material has its own reference level of zero energy setting at the top of the valence band, namely, the Γ_{15} .

On the absolute energy scale, the Γ_{15} energy $E_{\Gamma}^V(\text{GaAs})$ of the pure bulk GaAs is different from the Γ_{15} energy $E_{\Gamma}^V(\text{AlAs})$ of the pure bulk AlAs. The energy difference $\varepsilon = E_{\Gamma}^V(\text{GaAs}) - E_{\Gamma}^V(\text{AlAs})$ is defined as the *band offset*. Therefore, if we set $E_{\Gamma}^V(\text{AlAs}) = 0$ as the absolute zero energy when we use the matrix elements derived by Vogl *et al.*, all the five diagonal matrix elements $h_{\alpha\alpha}^{ii}$ for the pure bulk GaAs should be raised by this amount of the band offset ε , where i is either a Ga site or an As site.

In the formulation of Vogl *et al.*²² for pure bulk semiconductors, each 5×5 matrix at any single site i (with elements $h_{\alpha\beta}^{ii}$) is already diagonalized in terms of the Löwdin orbitals. For one such single site, let $E_l(\alpha, q)$ be the energy level of the α th Löwdin orbital on a q -type atom in the l th pure bulk semiconductor. The index l has the value $l=1$ for pure bulk AlAs or $l=2$ for pure bulk GaAs, and q can be either a cation ($q=c$) or an anion ($q=a$). Similarly, the elements $h_{\alpha\beta}^{ij}$ of the 5×5 matrix for an $\langle ij \rangle$ nearest-neighbor pair of an anion and a cation are more precisely specified as $V_l(\alpha, q; \beta, r)$, when the i th site in the l th pure semiconductor ($l=1$ for AlAs and $l=2$ for GaAs) is a q -type atom and the j th site an r -type atom. The values of all these matrix elements are listed in Table I including the band-offset correction.

TABLE I. Matrix element in units of eV for the sp^3s^* tight-binding band calculation. The subscript $l=1$ is for AlAs, and $l=2$ is for GaAs.

$E_l(\alpha, \beta)$	$l=1$	$l=2$
$E_l(s, a)$	-7.5273	-8.3431 + ε
$E_l(p, a)$	0.9833	1.0414 + ε
$E_l(s, c)$	-1.1627	-2.6569 + ε
$E_l(p, c)$	3.5867	3.6686 + ε
$E_l(s^*, a)$	7.4833	8.5914 + ε
$E_l(s^*, c)$	6.7267	6.7386 + ε
$V_l(\alpha, \beta, \gamma, \delta)$	$l=1$	$l=2$
$V_l(s, s)$	-6.6642	-6.4513
$V_l(x, x)$	1.8789	1.9546
$V_l(x, y)$	4.2919	5.0779
$V_l(s, a; p, c)$	5.1106	4.4800
$V_l(s, c; p, a)$	5.4965	5.7839
$V_l(s^*, a; p, c)$	4.5216	4.8422
$V_l(p, a; s^*, c)$	4.9950	4.8077

When we mix AlAs and GaAs to form an alloy, a heterojunction, or a MQW, each Al atom or Ga atom still has four nearest-neighbor As atoms, exactly the same local environment as in pure bulk GaAs and AlAs. Therefore, for i being an Al atom or a Ga atom the matrix elements $h_{\alpha\beta}^{ij}$ have the same values as given in Table I. However, the nearest neighbor of an As atom can have μ Al atoms and $4-\mu$ Ga atoms located at four different nearest-neighbor sites. In this case the matrix elements $h_{\alpha\beta}^{ii}$ are approximated as

$$h_{\alpha\beta}^{ii} = \frac{1}{4} [\mu E_1(\alpha, a) + (4-\mu) E_2(\alpha, a)] \delta_{\alpha\beta}. \quad (2)$$

Finally, since the lattice constants of pure GaAs and pure AlAs match well to each other, for a nearest-neighbor pair, the matrix elements $h_{\alpha\beta}^{ij}$ can be well approximated by those values given in Table I with negligible error.

The materials to be studied here have layer structures along the [001] direction. It is then more convenient to label the position of an atom by a layer index m and a position vector \mathbf{R}_i within the layer. In terms of this notation, i is expressed as (m, \mathbf{R}_i) , and $h_{\alpha\beta}^{ij}$ becomes $h_{\alpha\beta}^{mn}(\mathbf{R}_i, \mathbf{R}_j)$.

Let $|m\mathbf{R}_i, \alpha\rangle$ be the α th Löwdin orbital at (m, \mathbf{R}_i) . The eigenfunction of the system can then be written as $\sum_{m,i,\alpha} C_{\alpha}^m(\mathbf{R}_i) |m\mathbf{R}_i, \alpha\rangle$. The coefficients of linear combination satisfy the eigenvalue equation

$$\sum_{n,j,\beta} h_{\alpha\beta}^{mn}(\mathbf{R}_i, \mathbf{R}_j) C_{\beta}^n(\mathbf{R}_j) = E C_{\alpha}^m(\mathbf{R}_i). \quad (3)$$

Taking the Fourier transformation within the m th layer

$$C_{\alpha}^m(\mathbf{k}) = \frac{1}{\sqrt{N}} \sum_j C_{\alpha}^m(\mathbf{R}_j) \exp(i\mathbf{k} \cdot \mathbf{R}_j), \quad (4)$$

and define the matrix element

$$H_{\alpha\beta}^{mn}(\mathbf{k}, \mathbf{p}) = \frac{1}{N} \sum_{j,l} h_{\alpha\beta}^{mn}(\mathbf{R}_l, \mathbf{R}_j) \exp[i(\mathbf{k} \cdot \mathbf{R}_l - \mathbf{p} \cdot \mathbf{R}_j)], \quad (5)$$

(3) is then reduced to

$$\sum_{n,\beta,p} H_{\alpha\beta}^{mn}(\mathbf{k},\mathbf{p})C_{\beta}^n(\mathbf{p})=EC_{\alpha}^m(\mathbf{k}). \quad (6)$$

In an Al_xGa_{1-x}As random alloy, $h_{\alpha\beta}^{mn}(\mathbf{R}_l,\mathbf{R}_j)$ is not invariant with respect to lattice translations parallel to the interface, and so cannot be written as $h_{\alpha\beta}^{mn}(\mathbf{R}_l-\mathbf{R}_j)$. When the values of m , n , α , and β are fixed, the matrix element $h_{\alpha\beta}^{mn}(\mathbf{R}_l,\mathbf{R}_j)$ can take two values: one for the GaAs bond and the other for the AlAs bond. In the limit of long wavelength (small \mathbf{k}), it is reasonable to approximate $h_{\alpha\beta}^{mn}(\mathbf{R}_l,\mathbf{R}_j)$ by its mean value $\langle h_{\alpha\beta}^{mn}(\mathbf{R}_l,\mathbf{R}_j) \rangle$ averaged over these two possible values. In this case,

$$\begin{aligned} H_{\alpha\beta}^{mn}(\mathbf{k},\mathbf{p}) &\approx \frac{1}{N} \left[\sum_j e^{i(\mathbf{k}-\mathbf{p})\cdot\mathbf{R}_j} \right] \left[\sum_{\mathbf{R}} \langle h_{\alpha\beta}^{mn}(\mathbf{R}) \rangle e^{i\mathbf{k}\cdot\mathbf{R}} \right] \\ &= H_{\alpha\beta}^{mn}(\mathbf{k})\delta_{\mathbf{k},\mathbf{p}}, \end{aligned} \quad (7)$$

where $\mathbf{R}=\mathbf{R}_l-\mathbf{R}_j$, and

$$H_{\alpha\beta}^{mn}(\mathbf{k}) = \sum_{\mathbf{R}} \langle h_{\alpha\beta}^{mn}(\mathbf{R}) \rangle e^{i\mathbf{k}\cdot\mathbf{R}}. \quad (8)$$

The eigenvalue equation (6) becomes simply

$$\sum_{n,\beta} H_{\alpha\beta}^{mn}(\mathbf{k})C_{\beta}^n(\mathbf{k})=E(\mathbf{k})C_{\alpha}^m(\mathbf{k}). \quad (9)$$

When the microstructure and the material parameters of an Al_xGa_{1-x}As alloy sample are given, the above coupled equations will be solved with a block-decimation method.²⁴ However, one crucial input quantity to (9) is the mean value $\langle h_{\alpha\beta}^{mn}(\mathbf{R}) \rangle$. The correct way of taking the average depends on the microstructure orders in the sample, which is quite complicated and less understood at the present.²⁵

III. BLOCK DECIMATION WITH MICROSTRUCTURE ORDERINGS

We will solve (9) for each individual transverse \mathbf{k} vector. To simplify the presentation in the following, we will omit the \mathbf{k} in all \mathbf{k} -dependent quantities. Let \mathbf{C}^n be a five-component column vector with the α element C_{α}^n , and \underline{H}^{nm} a 5×5 matrix with the (α,β) element $H_{\alpha\beta}^{nm}$. Due to its nearest-neighbor-coupling property, (9) can be rewritten in the form of a vector equation

$$(\underline{H}^{nn}-\underline{E}\underline{I})\cdot\mathbf{C}^n+\underline{H}^{n,n-1}\cdot\mathbf{C}^{n-1}+\underline{H}^{n,n+1}\cdot\mathbf{C}^{n+1}=0, \quad (10)$$

where \underline{I} is a 5×5 unit matrix.

The vectors $\mathbf{C}^{n\pm 1}$ can be expressed from (10) as

$$\mathbf{C}^{n\pm 1} = -(\underline{H}^{n\pm 1,n\pm 1}-\underline{E}\underline{I})^{-1}\cdot(\underline{H}^{n\pm 1,n\pm 2}\cdot\mathbf{C}^{n\pm 2}+\underline{H}^{n\pm 1,n}\cdot\mathbf{C}^n). \quad (11)$$

Substituting $\mathbf{C}^{n\pm 1}$ into (10), it becomes

$$\begin{aligned} &\left[\underline{H}^{nn} - \sum_{\xi=\pm} \underline{H}^{n,n\xi 1}\cdot(\underline{H}^{n\xi 1,n\xi 1}-\underline{E}\underline{I})^{-1}\cdot\underline{H}^{n\xi 1,n} - \underline{E}\underline{I} \right] \cdot \mathbf{C}^n \\ &- \underline{H}^{n,n-1}\cdot(\underline{H}^{n-1,n-1}-\underline{E}\underline{I})^{-1}\cdot\underline{H}^{n-1,n-2}\cdot\mathbf{C}^{n-2} - \underline{H}^{n,n+1}\cdot(\underline{H}^{n+1,n+1}-\underline{E}\underline{I})^{-1}\cdot\underline{H}^{n+1,n+2}\cdot\mathbf{C}^{n+2} = 0. \end{aligned} \quad (12)$$

Equation (12) has exactly the same form as (10), and so a renormalization procedure can be established to solve the eigenvalue problem. This block-decimation method was introduced earlier²⁴ to renormalize the Green's-function equation of motion.

This kind of real-space renormalization has been commonly used to study the eigenproperties of disordered systems.²⁶⁻³¹ The final answer has to be derived numerically, and the configuration average over a large number of sizable random samples requires expensive computer time. Hence, instead of taking the exact configuration average, one uses the approximation of local averaging over the renormalized quantities at each step of decimation. The error so introduced drops rapidly when the spatial region for local average gets larger.³¹

For the system Al_xGa_{1-x}As alloy considered in this paper, the computation procedure is tremendously simplified because along the [001] direction every second plane is a pure As plane. Each As atom has four nearest-neighbor cations (Al or Ga), two at the left and two at the right side. If we know the probability of these four cation sites being occupied by the Al and the Ga atoms in a specific configuration, then the local average can be made on the renormalized matrices, which are

denoted as

$$\underline{W}^{nn} = \left\langle \left(\underline{H}^{nn} - \sum_{\xi=\pm} \underline{H}^{n,n\xi 1}\cdot(\underline{H}^{n\xi 1,n\xi 1}-\underline{E}\underline{I})^{-1}\cdot\underline{H}^{n\xi 1,n} \right) \right\rangle_{\text{LCA}} \quad (13)$$

and

$$\underline{W}^{n,n\pm 2} = -\langle \underline{H}^{n,n\pm 1}\cdot(\underline{H}^{n\pm 1,n\pm 1}-\underline{E}\underline{I})^{-1}\cdot\underline{H}^{n\pm 1,n\pm 2} \rangle_{\text{LCA}}, \quad (14)$$

where LCA means a local configuration average. After making the LCA, (12) has the simple form

$$(\underline{W}^{nn}-\underline{E}\underline{I})\cdot\mathbf{C}^n+\underline{W}^{n,n-2}\cdot\mathbf{C}^{n-2}+\underline{W}^{n,n+2}\cdot\mathbf{C}^{n+2}=0. \quad (15)$$

Let us assume that the n th plane is an As plane. Then, in (15) only the As planes are coupled after one step of decimation. If the distribution of the Al and the Ga atoms in each cation plane is completely random (R), then, all \underline{W}^{nn} are equivalent and all $\underline{W}^{n,n\pm 2}$ are equivalent. Consequently, (15) represents an effective regular tight-binding system consisting of only the anion planes, which can be solved analytically. Besides the

trivial R case, we will consider two possible phenomenological orderings for which (15) can also be solved analytically. One is the short-range order (SRO) *within each individual cation plane*, and the other is the long-range order (LRO) along the [001] direction such that the total Al concentration varies from layer to layer in the form of a particle-density wave.³² Both the SRO and the LRO situation were studied earlier.²³

From the definitions in (8), (14), and (15), the LCA is performed over four anion-cation bonds in $\langle h_{\alpha\beta}^{mn}(\mathbf{R}) \rangle e^{ik \cdot \mathbf{R}}$ with fixed α and β . For \underline{W}^{nn} the four bonds are between one As atom and its four nearest-neighbor cations: two in the $(n-1)$ th plane and two in the $(n+1)$ th plane. However, for $\underline{W}^{n,n\pm 2}$ the four bonds involve two As atoms: one in the n th plane and the other in the $(n\pm 2)$ th plane, and each As atom has two bonds with the two nearest-neighbor cation atoms in the $(n\pm 1)$ th plane. In the following we will analyze the LCA for the three cases.

A. Random alloy

In an $\text{Al}_x\text{Ga}_{1-x}\text{As}$ random alloy, the occupation probability at any cation site by an Al atom is $P(\text{Al})=x$, and by a Ga atom is $P(\text{Ga})=1-x$. For the two cations in the m th plane which are nearest neighbors to an As atom in the n th plane, let μ_m be the number of Al atoms. Then the local configuration probability (LCP) is

$$[P(\text{Al})]^{\mu_{n-1}+\mu_{n+1}}[P(\text{Ga})]^{4-\mu_{n-1}-\mu_{n+1}}$$

for calculating \underline{W}^{nn} , and is $[P(\text{Al})]^{2\mu_{n\pm 1}}[P(\text{Ga})]^{4-2\mu_{n\pm 1}}$ for calculating $\underline{W}^{n,n\pm 2}$.

B. Short-range order

Based on the thermal condition of sample growth, theoretical analysis³³ suggested the tendency of a phase segregation between the pure AlAs and the pure GaAs. Here we consider the first situation that the tendency of phase segregation does not produce a LRO along the [001] direction, but produces a SRO *within each individual cation plane*. The SRO assumes the form of a pair correlation between two cations which are next-nearest-neighbor pair (in the cation sublattice they are nearest-neighbor pair). For the cation pair in the m th plane, the correlation function is expressed as

$$P(K_m, L_m) = P(K_m)P(L_m)(1-\sigma) + \delta_{K_m L_m} P(K_m)\sigma, \quad (16)$$

where K_m and L_m can be either Al or Ga, and $\sigma < 1$ is the SRO parameter. We have further assumed the form $\sigma(x) = \gamma x(1-x)$ with a constant $\gamma < 4$.

In terms of the pair correlation, $P(K_{n-1}, L_{n-1})P(K_{n+1}, L_{n+1})$ should be the proper LCP used for calculating \underline{W}^{nn} , while $[P(K_{n\pm 1}, L_{n\pm 1})]^2$ for the calculation of $\underline{W}^{n,n\pm 2}$.

C. Long-range order

Next we consider the situation that the tendency of phase segregation results in a simple LRO in the cation

sublattice along the [001] direction. In the cation sublattice, the average Al concentration in a plane alternates between two values $x+\tau$ and $x-\tau$. Therefore the cation sublattice is further separated into two sublattices: the (+) sublattice with a planar Al concentration $x+\tau$, and the (-) sublattice with a planar Al concentration $x-\tau$. Since the Al concentration cannot be negative, we have $\tau \leq \tau_{\max} = x$ for $x \leq 0.5$, and $\tau \leq \tau_{\max} = 1-x$ for $x \geq 0.5$.

In each individual cation plane, the spatial distribution of the Al and the Ga atoms is completely random. Therefore the occupation probability at any cation site in the (\pm) sublattice by an Al atom is $P_{\pm}(\text{Al}) = x \pm \tau$, and by a Ga atom is $P_{\pm}(\text{Ga}) = 1 - (x \pm \tau)$. For the n th plane which is occupied by As atoms, let the $(n\pm 1)$ th plane be in the (\pm) sublattice. If the number of Al atoms in the $(n\pm 1)$ th plane is μ_{\pm} , then the LCP for calculating all \underline{W}^{nn} has only a single form

$$P_+(\text{Al})^{\mu_+} P_-(\text{Al})^{\mu_-} P_+(\text{Ga})^{2-\mu_+} P_-(\text{Ga})^{2-\mu_-}.$$

On the other hand, as a result of the finer sublattice structure in the cation sublattice, the LCP for calculating $\underline{W}^{n,n\pm 2}$ has two values $P_{\pm}(\text{Al})^{\mu_{\pm}} P_{\pm}(\text{Ga})^{2-\mu_{\pm}}$.

IV. BAND OFFSET

The characteristic feature of the LCP indicates that (15) is equivalent to the Schrödinger equation of a one-dimensional tight-binding Hamiltonian, either without a sublattice structure (for the random and the SRO cases), or with a sublattice structure (for the LRO case). Hence (15) can be solved analytically, using the matrix elements listed in Table I, and other input parameters such as the energy difference $\varepsilon = F_{\Gamma}^V(\text{GaAs}) - E_{\Gamma}^V(\text{AlAs})$ between the two valence-band maxima, the γ for the SRO, and the τ for the LRO. We have used a medium value of $\gamma = 1.5$ and a large value $\tau = \tau_{\max}$. The quantitative dependence of the final result on these parameter values will be discussed later. The measured value of ε is around 0.45–0.55 eV.^{2–6,34} If we fit the calculated band gap to the superlattice experimental data,^{35,36} the derived value of ε is about 0.4 eV. In our calculation, we have used three values $\varepsilon = 0.4, 0.5, \text{ and } 0.6$ eV.

Figure 2 shows the calculated band edges for $\varepsilon = 0.4$ eV as functions of the Al concentration in an $\text{Al}_x\text{Ga}_{1-x}\text{As}$ alloy. The three microstructure orderings are marked by R , SRO, and LRO in three panels. Due to the improved computation method of block decimation, the present result is different from the one derived earlier.²³

Knowing the band edges, the band-offset coefficient Q is then readily obtained from (1). At the presence of a LRO, the band folding caused by the finer sublattice structure in the cation sublattice makes the Γ point and the X point coincide.²³ Consequently, in this case the relevant band edges for calculating Q are the Γ_1 and Γ_{15} when $x \leq 0.5$, and X_1 and Γ_{15} when $x \geq 0.5$. However, for the cases of random alloy and SRO, what band edges are relevant to the calculation of Q is not so obvious when $x \geq 0.38$. For $\text{Al}_x\text{Ga}_{1-x}\text{As}$ with $x \geq 0.38$, the direct band gap is between Γ_{15} and Γ_1 , but the indirect

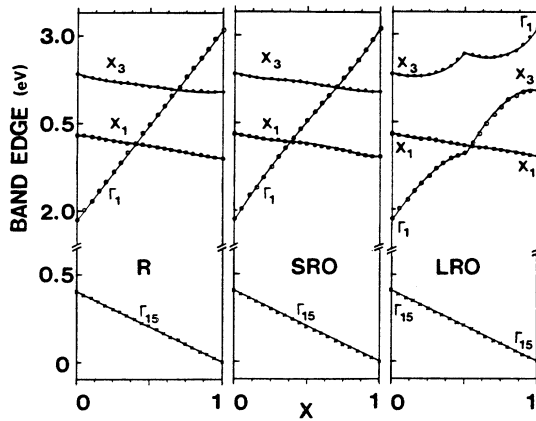


FIG. 2. Band edges of an $\text{Al}_x\text{Ga}_{1-x}\text{As}$ alloy with $\varepsilon=0.4$ eV. The three possible microstructure orderings in the cation subsystem are as follows: R for random distribution of the cations, SRO for short-range order within each cation plane, and LRO for long-range order between adjacent cation planes. For the case of LRO the symmetry labels are well defined only at $x=0$ and 1.

band gap is between Γ_{15} and X_1 . While the direct gap can be measured accurately³⁷⁻⁴⁰ with x as large as 0.8, accurate experimental determination of the indirect gap is not so easy. As we mentioned earlier, in our real-space renormalization procedure with the local configuration average, after the first block decimation the effective Hamiltonian becomes a regular tight-binding type. This method produces the same symmetry properties as those obtained by the virtual crystal approximation. Hence, in our work the optical transition probability between Γ_{15} and X_1 vanishes. On the other hand, the theoretical calculation of Ting and Chang⁴¹ yields a finite probability for the Γ_{15} -to- X_1 transition even for a random $\text{Al}_x\text{Ga}_{1-x}\text{As}$ alloy with $0 \leq x \leq 1$. Consequently, to calculate the Q for the cases of random alloy and SRO, we will use the band edges Γ_1 and Γ_{15} when $x \leq 0.38$, but will consider both the ($\Gamma_{15} \rightarrow \Gamma_1$) and the ($\Gamma_{15} \rightarrow X_1$) situations when $x \geq 0.38$.

Figure 3 shows the calculated Q for $\varepsilon=0.4, 0.5$, and 0.6 eV. If we use the direct band gap between Γ_{15} and Γ_1 , then the Q for a random alloy is a constant horizontal line, and the Q for the SRO is marked by open circles. In the region $x \geq 0.38$, if we use the indirect band gap between Γ_{15} and X_1 , then the Q for a random alloy and the Q for the SRO are hardly distinguishable, and are represented by the open diamonds. In the region $x \geq 0.5$, these open diamonds almost coincide with the Q of the LRO case (open squares). While the effect of SRO on Q is very weak, the effect of LRO on the band-offset coefficient is stronger in the vicinity of $x \approx 0.38$.

In particular, when $\varepsilon=0.5$ eV, both the random alloy

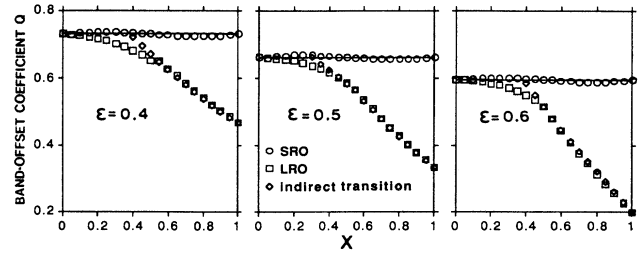


FIG. 3. The band-offset coefficient of an $\text{Al}_x\text{Ga}_{1-x}\text{As}$ alloy with $\varepsilon=0.4, 0.5$, and 0.6 eV. The open circles and the horizontal straight lines (for the random alloy) are derived with the direct band gap between Γ_{15} and Γ_1 . In the region $x \geq 0.38$, the open diamonds are for both the SRO and the random alloy, calculated with the indirect band gap between Γ_{15} and X_1 .

and the SRO yield a value of Q around 0.66. This result fits well to the existing experimental observations.^{2-6,8,34}

V. REMARKS

Although the present result derived from the block-decimation method is much improved over the previous one,²³ the local configuration average (LCA) is performed on a small cluster. It has been shown in Ref. 31 that more accurate results can be obtained if we use a larger cluster for LCA. Hence the present work should be extended along this direction. Recently, the distribution probability of various types of clusters in an $\text{Al}_x\text{Ga}_{1-x}\text{As}$ alloy has been investigated in detail.²⁵ By incorporating this valuable information into our block-decimation scheme, we automatically introduce the correct correlation between atoms in different cation planes, which has been ignored in the present calculation.

Finally, we should mention that for the case of SRO, the band-offset coefficient Q is insensitive to the value of the short-range-order parameter γ . The LRO curves in Fig. 3 are derived with the strongest possible long-range ordering $\tau=\tau_{\text{max}}$. If the LRO is very weak, we found that for $x \leq 0.38$ the Q value deviates only slightly from the constant Q value for the random alloy. Since the formation of LRO requires the diffusion of cations through anion planes, judging from the growth condition of the $\text{Al}_x\text{Ga}_{1-x}\text{As}$ sample, it seems that the existence of a strong LRO is unlikely. If this argument is acceptable, our calculation shown in Fig. 3 agrees well with experiment.

ACKNOWLEDGMENTS

One of us (Y.F.) is grateful to Dr. Q. Chen for valuable discussions on various aspects of semiconductor experiments. This work was financially supported by the Swedish Natural Science Research Council under Grant No. F-FU 3996-306.

- ¹H. Kroemer, W.-Y. Chien, J. S. Harris, Jr., and D. D. Edwall, *Appl. Phys. Lett.* **36**, 295 (1980).
- ²W. I. Wang and F. Stern, *J. Vac. Sci. Technol. B* **3**, 1280 (1985).
- ³J. Batey and S. L. Wright, *J. Appl. Phys.* **59**, 200 (1986).
- ⁴J. Menendez, A. Pinczuk, D. J. Werder, A. C. Gossard, and J. H. English, *Phys. Rev. B* **33**, 8863 (1986).
- ⁵P. Dawson, K. J. Moore, and C. T. Foxon, *Proc. SPIE* **792**, 208 (1987).
- ⁶D. J. Wolford, in *Proceedings of the 18th International Conference on the Physics of Semiconductors, Stockholm, 1986*, edited by O. Engström (World Scientific, Singapore, 1986), p. 1115.
- ⁷R. Dingle, W. Wiegmann, and C. H. Henry, *Phys. Rev. Lett.* **33**, 827 (1974).
- ⁸R. C. Miller, D. A. Kleinman, and A. C. Gossard, *Phys. Rev. B* **29**, 7085 (1984).
- ⁹R. L. Anderson, *Solid State Electron.* **5**, 341 (1962).
- ¹⁰J. O. McCaldin, T. C. McGill, and C. A. Mead, *J. Vac. Sci. Technol.* **13**, 802 (1976).
- ¹¹W. A. Harrison, *J. Vac. Sci. Technol.* **14**, 1016 (1977).
- ¹²W. R. Frensley and H. Kroemer, *Phys. Rev. B* **16**, 2642 (1977).
- ¹³W. E. Pickett, S. G. Louie, and M. L. Cohen, *Phys. Rev. B* **17**, 815 (1978).
- ¹⁴M. T. Yin and M. L. Cohen, *Phys. Rev. Lett.* **45**, 1004 (1980).
- ¹⁵J. Ihm and J. D. Joannopoulos, *Phys. Rev. B* **24**, 4191 (1981).
- ¹⁶J. Tersoff, *Phys. Rev. B* **30**, 4874 (1984); F. Floures and C. Tejedor, *J. Phys. C* **12**, 731 (1979) and references therein.
- ¹⁷M. J. Galdas, A. Fazzio, and A. Zunger, *Appl. Phys. Lett.* **45**, 671 (1984).
- ¹⁸A. Zunger, *Phys. Rev. Lett.* **54**, 849 (1985).
- ¹⁹S. Massidda, B. I. Min, and A. J. Freeman, *Phys. Rev. B* **35**, 9871 (1987).
- ²⁰S. H. Wei and A. Zunger, *Phys. Rev. Lett.* **59**, 144 (1987).
- ²¹S. B. Zhang, D. Tomanek, S. G. Louie, M. L. Cohen, and M. S. Hybertsen, *Solid State Commun.* **66**, 585 (1988).
- ²²P. Vogl, H. P. Hjalmarson, and J. D. Dow, *J. Phys. Chem. Solids* **44**, 365 (1983).
- ²³Y. Fu, K. A. Chao, and R. Osorio, *Phys. Rev. B* **40**, 6417 (1989).
- ²⁴Y. Liu, R. Riklund, and K. A. Chao, *J. Phys. C* **17**, L843 (1984).
- ²⁵L. G. Ferreira, S. H. Wei, and A. Zunger, *Phys. Rev. B* **40**, 3197 (1989).
- ²⁶H. Aoki, *Solid State Commun.* **31**, 999 (1979).
- ²⁷B. Koiller, M. O. Robbins, M. A. Davidovich, and C. E. T. Goncalves da Silva, *Solid State Commun.* **45**, 955 (1983).
- ²⁸M. O. Robbins and B. Koiller, *Phys. Rev. B* **27**, 7703 (1983).
- ²⁹B. W. Southern, A. A. Kumar, and J. A. Ashraff, *Phys. Rev. B* **28**, 1785 (1983).
- ³⁰C. Wiecko and E. Roman, *Phys. Rev. B* **30**, 1603 (1984).
- ³¹Y. Liu and K. A. Chao, *Phys. Rev. B* **33**, 1010 (1986).
- ³²T. S. Kuan, T. F. Kuech, W. I. Wang, and E. L. Wilkie, *Phys. Rev. Lett.* **54**, 201 (1985).
- ³³S. Ciraci and I. P. Batra, *Phys. Rev. Lett.* **58**, 2114 (1987).
- ³⁴W. I. Wang, *Solid State Electron.* **29**, 133 (1986).
- ³⁵A. C. Gossard, P. M. Petroff, W. Wiegmann, R. Dingle, and A. Savage, *Appl. Phys. Lett.* **29**, 323 (1976).
- ³⁶B. A. Vojak, W. D. Laidig, N. Holonyak, M. D. Camras, J. J. Coleman, and P. D. Dapkus, *J. Appl. Phys.* **53**, 621 (1981).
- ³⁷P. J. Pearah, W. T. Masselink, J. Klem, T. Henderson, H. Morkoç, C. W. Litton, and D. C. Reynolds, *Phys. Rev. B* **32**, 3857 (1985).
- ³⁸T. F. Kuech, D. J. Wolford, E. Veuhoff, V. Deline, P. M. Mooney, R. Potemski, and J. Bradley, *J. Appl. Phys.* **62**, 632 (1987).
- ³⁹T. F. Kuech, D. J. Wolford, R. Potemski, J. A. Bradley, K. H. Kelleher, D. Yan, J. P. Farrell, P. M. S. Lesser, and F. H. Pollak, *Appl. Phys. Lett.* **51**, 505 (1987).
- ⁴⁰C. Bosio, J. L. Staehli, M. Guzzi, G. Burri, and R. A. Logan, *Phys. Rev. B* **38**, 3263 (1988).
- ⁴¹D. Z.-Y. Ting and Y.-C. Chang, *Phys. Rev. B* **30**, 3309 (1984).